Baghdad Science Journal

Volume 23 | Issue 1 Article 12

1-1-2026

Low Temperature AC Photoelectrochemical Etching of Si-doped n-type GaN: Nanostructure Fabrication for Enhanced MSM Photodetector Performance

Nur Iwani Nor Izaham
Faculty of Applied Sciences, Universiti Teknologi MARA, Shah Alam, Selangor, Malaysia, nuriwani1999@gmail.com

Ainorkhilah Mahmood
Department of Applied Sciences, Universiti Teknologi MARA Cawangan Pulau Pinang, Permatang Pauh, Malaysia, ainorkhilah_sp@uitm.edu.my

Rosfariza Radzali
Electrical Engineering Studies, College of Engineering, Universiti Teknologi MARA Cawangan Pulau Pinang, Permatang Pauh, Malaysia, rosfariza074@uitm.edu.my

Alhan Farhanah Abd Rahim
Electrical Engineering Studies, College of Engineering, Universiti Teknologi MARA Cawangan Pulau Pinang, Permatang Pauh, Malaysia, alhan570@uitm.edu.my

Nur Maizatul Azra Mothtar
Faculty of Health Sciences, Universiti Teknologi MARA Cawangan Pulau Pinang, Kepala Batas, Malaysia, nurmaizatul038@uitm.edu.my

See next page for additional authors

How to Cite this Article

Izaham, Nur Iwani Nor; Mahmood, Ainorkhilah; Radzali, Rosfariza; Rahim, Alhan Farhanah Abd; Mothtar, Nur Maizatul Azra; Ooi, Mahayatun Dayana Johan; and Ahmed, Naser Mahmoud (2026) "Low Temperature AC Photoelectrochemical Etching of Si-doped n-type GaN: Nanostructure Fabrication for Enhanced MSM Photodetector Performance," *Baghdad Science Journal*: Vol. 23: Iss. 1, Article 12.
DOI: https://doi.org/10.21123/2411-7986.5138

Low Temperature AC Photoelectrochemical Etching of Si-doped n-type GaN: Nanostructure Fabrication for Enhanced MSM Photodetector Performance

Authors

Nur Iwani Nor Izaham, Ainorkhilah Mahmood, Rosfariza Radzali, Alhan Farhanah Abd Rahim, Nur Maizatul Azra Mothtar, Mahayatun Dayana Johan Ooi, and Naser Mahmoud Ahmed

BAGHDAD SCIENCE JOURNAL 2026;23(1):151–164

Scan the QR to view the full-text article on the journal website

SPECIAL ISSUE ARTICLE

Low Temperature AC Photoelectrochemical Etching of Si-doped n-type GaN: Nanostructure Fabrication for Enhanced MSM Photodetector Performance

Nur Iwani Nor Izaham [1], Ainorkhilah Mahmood [2,*], Rosfariza Radzali [3], Alhan Farhanah Abd Rahim [3], Nur Maizatul Azra Mokhtar [4], Mahayatun Dayana Johan Ooi [5], Naser Mahmoud Ahmed [6]

[1] Faculty of Applied Sciences, Universiti Teknologi MARA, Shah Alam, Selangor, Malaysia
[2] Department of Applied Sciences, Universiti Teknologi MARA Cawangan Pulau Pinang, Permatang Pauh, Malaysia
[3] Electrical Engineering Studies, College of Engineering, Universiti Teknologi MARA Cawangan Pulau Pinang, Permatang Pauh, Malaysia
[4] Faculty of Health Sciences, Universiti Teknologi MARA Cawangan Pulau Pinang, Kepala Batas, Malaysia
[5] School of Physics, Universiti Sains Malaysia, Minden, Malaysia
[6] Laser and Optoelectronics Engineering Department, Dijlah University College, Baghdad, Iraq

ABSTRACT

This study has investigated the fabrication of porous Si-doped gallium nitride (GaN) using low-temperature alternating current photoelectrochemical (ACPEC) etching at varying etching durations for MSM photodetector applications. The structural and optical characteristics of the porous GaN samples were examined using a 400 W high-pressure mercury-vapour lamp (Hg-HPVL) and 4% KOH electrolyte with 50 Hz of 100 mA alternating current (AC). Current-voltage (I-V) measurements were conducted to analyse the platinum-deposited GaN for MSM photodetector performance. FESEM micrographs of the etched samples revealed coral-like and nano-tunnel pore formations, while AFM topography showed a significant increase in surface roughness compared to in the as-grown samples. The minimal difference between the average pore depth and RMS surface roughness values indicated successful fabrication of a nano-coral structure with a uniform, evenly distributed depth. Raman spectroscopy of the etched samples showed shifts in the A_1 (LO) peak wavelengths and an increase in the E_2 (high) peak intensity across different etching times compared to in the as-grown samples. XRD analysis further confirmed the presence of dislocation density along the x- and z-axis across all samples. Additionally, I-V measurements of the MSM photodetector demonstrated a higher current in all porous samples compared to in as-grown samples under various environmental conditions. These findings indicated that low-temperature ACPEC etching could be an effective approach for fabricating porous GaN with higher currents for photodetector applications.

Keywords: Low temperature, MSM photodetector, Nanostructure, Photoelectrochemical, Si-doped GaN

Introduction

Porous semiconductors have received extensive attention in recent years, owing to their distinct optical properties when compared to bulk materials, as well as their potential uses in optoelectronics, chemical sensing, and biological sensing.[1–4] Their high surface area, shift of band gap, luminescence intensity enhancement, and efficient photoresponse when pores are formed could be tailored to fabricate new sensing

Received 28 February 2025; revised 8 August 2025; accepted 17 August 2025.
Available online 1 January 2026

* Corresponding author.
E-mail addresses: nuriwani1999@gmail.com (N. I. Nor Izaham), ainorkhilah_sp.uitm.edu.my (A. Mahmood), rosfariza074@uitm.edu.my (R. Radzali), alhan570@uitm.edu.my (A. F. Abd Rahim), nurmaizatul038@uitm.edu.my (N. M. A. Mokhtar), mahayatun@usm.my (M. D. Johan Ooi), naser.mahmoud@duc.edu.iq (N. M. Ahmed).

International Conference on Discoveries in Applied Sciences and Applied Technology (DASAT2025)
https://doi.org/10.21123/2411-7986.5138

devices.[5] Porous gallium nitride (GaN) research has sparked interest because of its unique properties, for example, porous GaN could decrease threading dislocations and accommodation strain.[6] Dry and wet etching techniques are used to create porous GaN. Dry etching techniques, such as reactive ion etching (RIE), inductively coupled plasma (ICP), and a hybrid of these two techniques, known as inductively coupled plasma reactive ion etching (ICP-RIE), could cause surface damages and they lack the desired selectivity for morphology, dopant, and composition.[7] On the other hand, wet etching techniques, such as electroless etching, direct current photoelectrochemical (DCPEC) etching, and alternating current photoelectrochemical (ACPEC) etching are cost effective, as well as sustainable methods without the use of hazardous gases, harsh chemicals, and high power.[8–11] Electroless etching is technically straightforward, cost-effective, and extensively applicable to both conductive and insulating substrates.[12] This method, however, makes homogeneous pore size and distribution nearly impossible to achieve.[13] The most practical wet etching methods for creating porous GaN are DCPEC and ACPEC etching. One of the common electrolytes used for etching is potassium hydroxide (KOH). This electrolyte is great for controlling the reaction kinetics during etching to achieve the desired etching rates and to maintain the quality of the etched GaN. In DCPEC etching, the KOH electrolyte being consumed during the chemical reactions in the pores could cause the concentration of the electrolyte in the vicinity of the semiconductor electrolyte interface (SEI) to decrease, which may reduce the effectiveness of the etching process.[14] Bubbles have been observed at the surface of GaN during DCPEC etching due to N_2 development, thus delaying the etching process and resulting in shallow pores.[15]

Etching conditions or temperature during the etching process could also affect the creation of porous GaN, even though it could be synthesised at room temperature. However, heat transfer from the high-power UV lamp or high-pressure mercury-vapour lamp (HPVL) during the etching process could increase the temperature of the etching system and potentially cause the electrolyte to vaporise. The etching activity and rate could reduce because of the aforementioned issues, resulting in GaN with non-uniform pores and poor porosity.[14] Furthermore, the porous GaN samples generated using this method was expected to have a low density and a low surface area-to-volume ratio.[16]

Porous GaN is an anisotropic material with a high surface-to-volume ratio at low temperatures. Low-temperature ACPEC etching is a technique that uses light-induced electrons and holes to aid electrochemical processes in semiconductors that are in contact with an electrolyte. In low-temperature ACPEC etching, the etching of GaN occurs only at the tip of the pores, where the electric field of the surface charge region (SCR) is locally amplified. Etching begins at specified initiation sites and would eventually evolve into the GaN layer for steady-state pore growth.[15,17] Thus, when the etching rate is increased at a low temperature, the grain boundaries will be etched significantly slower than the centres of the crystals. Therefore, the pore structure could be constrained to a smaller size. ACPEC utilises AC as the power source for the PEC etching process. Hole generation at the SEI refers to the creation of holes, which is the positive charge carrier at the interface between GaN and KOH during PEC processes, as shown in Fig. 1.

When light illuminates the surface of GaN, it excites electrons from the valence band to the conduction band, creating holes in the valence band, as shown in Fig. 1(a). The AC electric field in the space charge region (SCR) assists in separating these carriers, with holes moving towards the surface, enabling the oxidation of GaN and initiating the etching process, as shown in Fig. 1(b). The oxide layer of Ga_2O_3 forms on the GaN surface and then, it experiences oxide dissolution when it dissolves into the KOH electrolyte.

This dissolution exposes the underlying GaN surface for continued etching, allowing the process to proceed smoothly. During the etching process, N_2 gas and ions, such as Ga^{3+} and O^{2-} were released. Photogenerated holes are driven to the interface for oxidation reaction during the anodic half-cycle, as seen in Fig. 1(d), while the photogenerated electrons diffuse into the GaN bulk. They are then transferred to the counter electrode via the external circuit, driven by voltage bias and band bending. As shown in Eqs. (1) and (2), holes on the GaN surface could contribute towards the oxidation of GaN to generate Ga_2O_3 when N_2 gas is evaluated.[18]

$$2GaN + 6h^+ \rightarrow 2Ga^{3+} + N_2 \quad (1)$$

$$2GaN + 6OH^- + 6h^+ \rightarrow Ga_2O_3 + 3H_2O + N_2 \quad (2)$$

The electrons contribute to the reduction of hydrogen during the cathodic half-cycle of the alternating current photoelectrochemical etching by evaluating H_2 gas from the platinum counter-electrode during the ACPEC etching process. Due to N_2 evolution, bubbles may be observed at the surface of GaN during PEC etching, which could slow down the etching process, resulting in shallow pores. Other than N_2 gas, ions such as Ga^{3+} and O^{2-} may also be produced. AC may reduce bubbles on the GaN surface by periodically reversing the electric field. This reversal

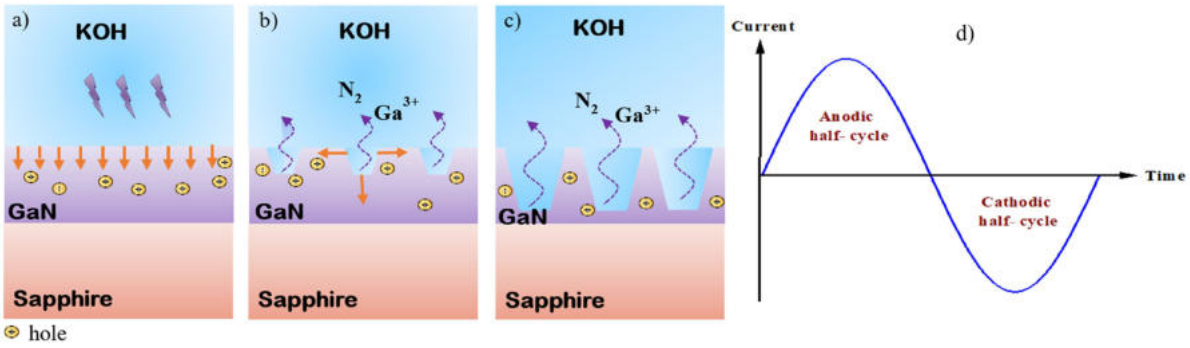

Fig. 1. Anodization at SEI of GaN and KOH at a) light incident on GaN, b) etching process occurs, c) etching penetrating deeper and d) Sinusoidal wave of AC.

induces the oscillation of ions and charged species in the solution, which would help reduce N_2 bubbles and prevent ions from blocking the active surfaces, or triggering undesired recombination reactions. The movement generated by the alternating electric field may prevent the bubbles and ions from accumulating. This enhances the etching process and allows it to proceed smoothly and uniformly. When gas bubbles and ions are reduced, fresh KOH molecules are free to react with the GaN surface, thus preserving the KOH concentration at constant SEI.[19]

Instead of using a common direct current, a sinusoidal alternating current with a frequency of 50 Hz was used in this study to establish homogeneity and porosity of porous GaN layers.[19] The electrochemical behaviour during ACPEC etching was strongly influenced by both the applied AC frequency and etching duration. At the low frequency of 50Hz used in this study, the alternation of bias provided sufficient time within each half-cycle for controlled photo-assisted oxidation and oxide dissolution, thus facilitating uniform pore initiation and propagation.[19] This balance between light-induced oxidation and chemical dissolution could lead to a porous morphology with minimal lattice damage.[20] Low temperature serves as a surface treatment for GaN, preventing the heat generated by high-power light sources, such as UV or polychromatic light, from impacting the SCR. The combination of low temperature and AC, which incorporate both cathodic and anodic cycles, could significantly reduce the likelihood of electron-hole pair recombination. The literature review showed that the fabrication of porous Si-doped GaN via low-temperature ACPEC etching has not been reported. Consequently, this research aimed to prepare porous Si-doped GaN via ACPEC etching at a low temperature, anticipating improvements in pore uniformity and porosity that could lead to a higher surface area-to-volume ratio. Porous GaN with increased capabilities has the potential to be employed in metal-semiconductor-metal (MSM) photodetectors. Thin films have been widely used for photodetection across the electromagnetic spectrum, with GaN being especially good at detecting UV and visible light.[21] Thus, this study has also fabricated MSM photodetector to ensure that the porous structure created using this method could produce a high-performance photodetector.

Materials and methods

This study employs two (2) inch in diameter Si-doped n-type GaN wafers grown via the Metal Organic Chemical Vapour Deposition (MOCVD) on one side of the polishing sapphire substrate, as shown in the schematic diagram in Fig. 2(a). The thickness of the GaN thin film was 5 μm. The GaN wafer was cut into 1 $\times$ 1 cm pieces using a diamond wafer cutter. This study has also employed a low-temperature AC photoelectrochemical etching technique to prepare porous GaN samples using three (3) key steps, namely pre-etching, low temperature ACPEC etching, and post-etching.

GaN is an extremely stable material that does not easily oxidises. However, GaN tends to react with native oxides and other particles on the surface of the GaN wafer and form Ga_2O_3 that could interrupt the etching process. To eliminate these oxides, the sample was immersed in ammonium (NH_3) solution for eight (8) min to remove any organic residue, followed by hydrofluoric acid (HF) solution for 20 sec to remove the native oxide. Then, the sample was cleaned by being boiled in an aqua regia solution for 5 min at 80 °C to remove any metal impurities. Each cleaning step was followed by rinsing with deionised (DI) water. The sample is wrapped using an aluminium (Al) sticker, with a small hole of 0.8 cm in diameter to allow the enhancement of electrical contact between the electrolyte and GaN surface, as shown in Fig. 2(b).

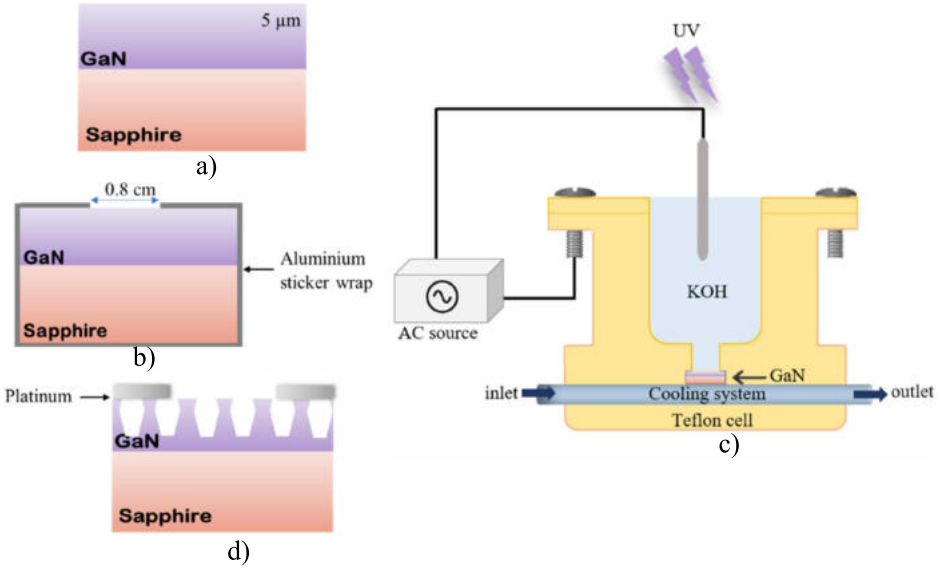

Fig. 2. Schematic diagram of a) Si-doped GaN sample, b) wrap contact, c) ACPEC etching at low temperature and d) MSM photodetector.

This step resulted in an ohmic contact for the sample with an etching area of 0.503 cm^2. The schematic diagram of the low-temperature ACPEC etching is shown in Fig. 2(c). Then, the sample was positioned under the O-ring and placed on top of the cooling system. The initial temperature of the circulation system was 20 ˚C. A temperature sensor was employed to monitor the etching temperature at 10 min intervals, with the recorded temperatures ranging between 9and 12˚C throughout the etching process. An AC of 100 mA with 50 Hz frequency was used and monitored via a clamp meter to avoid the risk of clipping incident during the process.[22] Other important parameters included a high-pressure mercury-vapour lamp (Hg-HPVL) as the light source, platinum (Pt) as the counter electrode, and 4% of potassium hydroxide (KOH) solution as the etchant. The manipulated variable in this study was the etching duration, with increasing 15 min durations starting at 45 min; thus, the etching durations of 45, 60, 75, and 90 min were chosen, with reference to prior studie s.[10,23–25] A short 45-min etching duration has been shown to be sufficient for producing a porous structure, while prolonged etching durations, for example, 90 min, have been reported to yield high-quality porous structures. The cooling system was turned on for 5 min before starting the PEC to ensure that the GaN wafer was in a thermal equilibrium as the cooling fluid flowed beneath the sapphire substrate of GaN. The sample was rinsed and immersed in an ultrasonic bath filled with DI water for post-etching. Only one sample, with no repetition, was fabricated for each etching condition. However, multiple analysis spots were selected within the same etched area of 0.503 cm^2 for characterisation to ensure representative and reliable measurements.

The surface morphology of the samples was analysed using an Extreme High-Resolution Field-Emission Scanning Electron Microscope (XHR-FESEM, FEI Verious 460L, United States, 2015). For porosity estimation, this study utilised grayscale thresholding analysis on top-view FESEM images using ImageJ software. To improve reliability, measurements were performed on three different regions of each sample, and the average porosity along with the standard deviation was reported. Surface roughness and pore depth with the scan area of 5 × 5 μm were analysed using an Atomic Force Microscope (AFM) (Dimension Edge, Bruker, German, 2011). To ensure consistency in pore depth measurements, line scans were performed at 10 different locations within a 5 × 5μm porous region using the Nanoscope Analysis software. The average depth from these scans was used as a representative value for each sample. Although this method did not yield absolute pore depths, it provided a reliable basis for comparative analysis of surface morphology across different etching durations. A Raman Spectrometer (Renishaw inVia Raman Microscope) was used in this study to analyse the optical characteristics of the samples. The crystalline properties of the GaN film was identified using a High Resolution X-Ray Diffractometer (HR-XRD), model Bruker D8 Discovery, with $\lambda = 1.5406$ Å of Cu-Kα1. The phase analysis (2θ scan mode) and rocking curve (ω scan mode) were performed. After the characterisation analysis, MSM photodetectors are fabricated by depositing Pt on top of GaN samples,

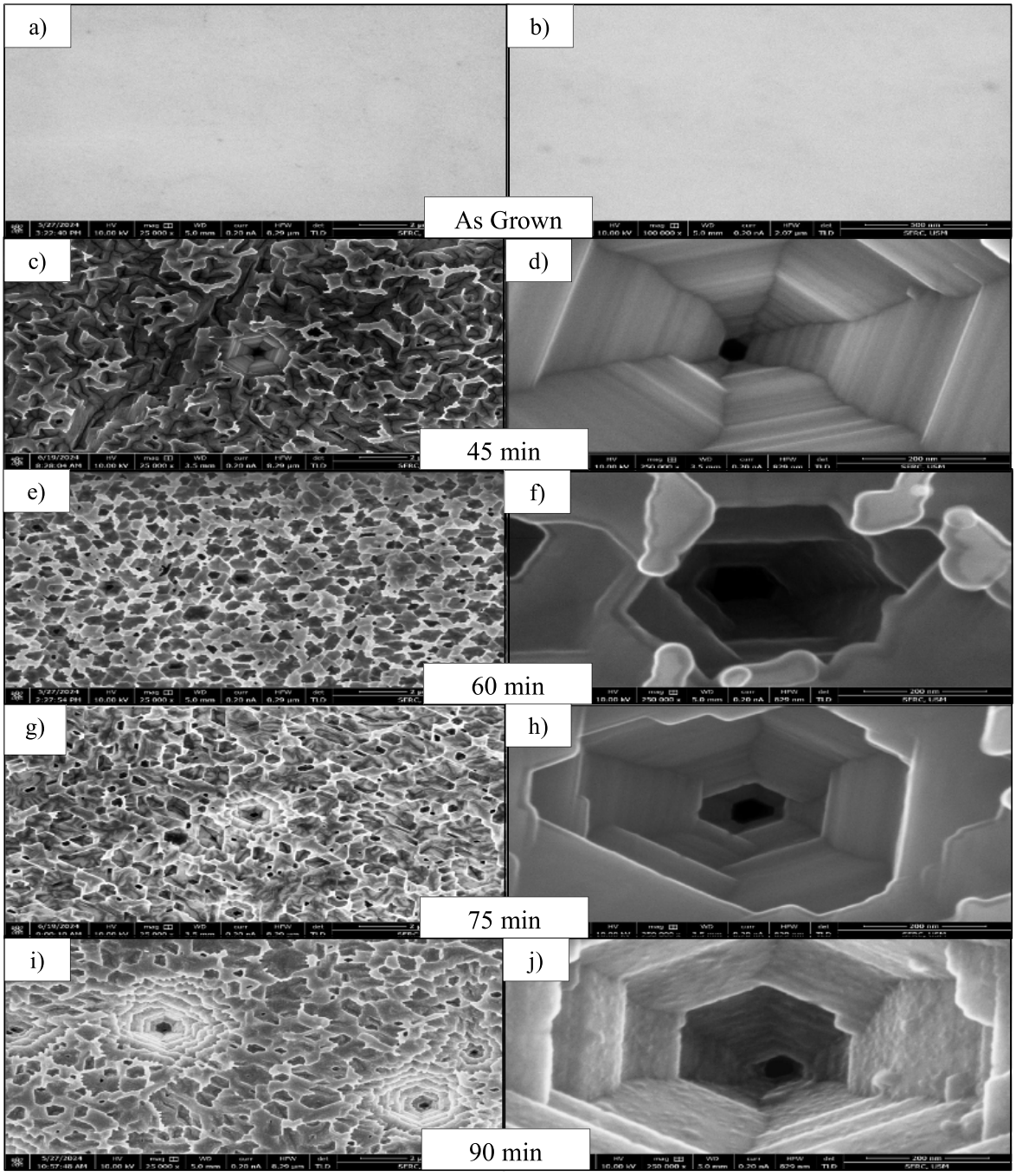

Fig. 3. FESEM images of as grown and porous GaN sample under different etching durations at 2μm of (a, c, e, g, i) and 200 nm of (b, d, f, h, j).

as seen in Fig. 2(d), using an E-Beam Evaporator, model ULTECH SEE-5S (metal). The deposition was conducted under 5 $\times$ 10^7 Torr of pressure at room temperature with substrate rotation of 100 rpm. The deposition rate was approximately 0.5 Å/s and the thickness of Pt was 100 nm. As-grown and optimised porous Si-doped GaN samples undergoing current-voltage (I-V) characterisation under different light illuminations were included to investigate the effectiveness of this method. The optimised sample was chosen based on the morphological, structural, topographical, optical enhancements, and crystalline quality of the sample.

Results and discussion

The top oblique FESEM images of Si-doped GaN etched under different durations are illustrated in Fig. 3(a) to 3(i). Fig. 3(a, c, e, g, and i) show the images at 25k magnification, while Fig. 3(b, d, f, h, and

j) show the images at the high magnification of 250k. The as-grown samples showed a level surface with no pores. When the current was set to 100 mA, all porous samples showed a similar network morphology with nanocoral-like pores. At higher magnifications, the morphology revealed deeper pores that penetrated deep into the GaN layer, forming nanotunnel-like pores. Fig. 3 also shows differences in pore size and porosity for all porous samples at 25k magnification. The 60-min sample showed the highest porosity at 59.27%, followed by the 90-, 75-, and 45-min samples with porosity at 58.32%, 57.33%, and 53.94%, respectively. This result may be due to the 60-min sample having a uniformly distributed pore shape and pore size. It was observed that the pore sizes of these samples continued to increase as the etching duration was increased. Another research obtained similar morphology when the etching duration was increased.[26]

A similar observation was also reported by Zhang et al. who obtain the foam like GaN structure with comparable pore pattern.[27] This study suggests that etching at different etching durations affected the pore morphology, including the pore size, pore shape, and percentage porosity.

The Si-doped GaN samples were subjected to an AFM analysis, with a scanning area of 5 × 5 μm in their as-grown state, and after being etched at various durations to create nanoporous structures. Fig. 4(a, c, e, g, and i) display 2D images on the left, and Fig. 4(b, d, f, h, and j) show 3D images on the right for each sample.

The as-grown sample has the lowest Root Mean Square (RMS) surface roughness, measuring at 2.2 nm, due to its relatively uniform surface, with a distribution of hillocks and no detectable cavities.[20] This result was consistent with the corresponding FESEM images and porosity data. The 2D data for porous samples matched the findings observed in FE-SEM images that showed the nanocoral-like pores. Fig. 5(a) presents a graph that illustrates the correlation between the estimated porosity obtained from the FESEM images and the RMS surface roughness obtained from the AFM analysis, as a function of etching duration. This graph demonstrated that surface roughness was not directly influenced by porosity. The 45-min sample has the highest surface roughness, measuring at 70.6 nm. The reduction in surface roughness starting from 45-min of etching may be attributed to the coalescence and reorganisation of the pore structure, whereby the merging of adjacent pores reduced surface irregularities and resulted in a smoother surface.[28] The relationship between pore depth and RMS value, as displayed in Fig. 5(b), shows no significant difference, which indicates that the pore depth is almost uniform across the samples. This observation proved that the porous structure has a uniform morphology and average pore depth.

The structural characteristics of the as-grown and porous Si-doped GaN films were further analysed using HR-XRD. The phase analysis of the 2θ scan range from 30° to 80°, as illustrated in Fig. 6, reveals the presence of hexagonal GaN phases oriented in the (0002) and (0004) planes (International Centre of Diffraction Data (ICDD) file no. 00-050-0792) across all GaN samples, along with diffraction peaks corresponding to sapphire (ICDD file no. 01-073-1512). This could be due to the GaN surface interacting with oxygen, leading to the formation of Ga_2O_3.The sapphire substrates in the examined films were the source of the sapphire peak detection. The detection of sapphire substrate could be attributed to imperfect cutting and polishing, resulting in a minor misalignment between the substrate surface and its crystalline planes.[29] An extra diffraction peak linked to β-Ga2O3 (ICDD file no. 01-074-1776) was also observed in the 60-min sample. The crystalline quality of the Si-doped GaN samples is analysed using the rocking curve analysis for the omega scans of the 0002 and $10\bar{1}2$ orientations, as illustrated in Fig. 7(a) and 7(b), respectively. The scan results, including peak position, full width half minimum (FWHM), and calculated interplanar spacing (d) using Eq. (3), are shown in Table 1.[16]

$$n\lambda = 2d\sin\theta \tag{3}$$

Where d is interplanar spacing, the reflection order is n = 1, incident wavelength of 1.5406 Å of Cu-Kα_1, and θ incident angle of 90°.

Despite having varied FWHMs, all samples displayed peaks at approximately 17° for the symmetric scan mode and at approximately 23° for the asymmetric mode. The 90-min sample has the lowest FWHM value of 0.0822° for the symmetric plane, whereas the 75-min sample has the lowest value of 0.1085° for the asymmetric plane. A decreased FWHM value could indicate enhanced crystallinity in the material.[30] Based on the data in Table 1, the lattice constant and dislocation density are computed and displayed in Table 2. Lattice constants, c and a, are calculated using Eqs. (4) and (5), respectively:[16]

$$c = \frac{\lambda l}{2sin\theta} \tag{4}$$

$$\frac{1}{d^2} = \frac{4}{3}\frac{h^2 + k^2 + hk}{a^2} + \frac{l^2}{c^2} \tag{5}$$

where c is the lattice constant along the z-axis, a is the lattice constant along the x-axis, while h, k, and l are the Miller indices, with incident wavelength of 1.5406 Å of Cu-Kα1 and θ incident angle. The linear

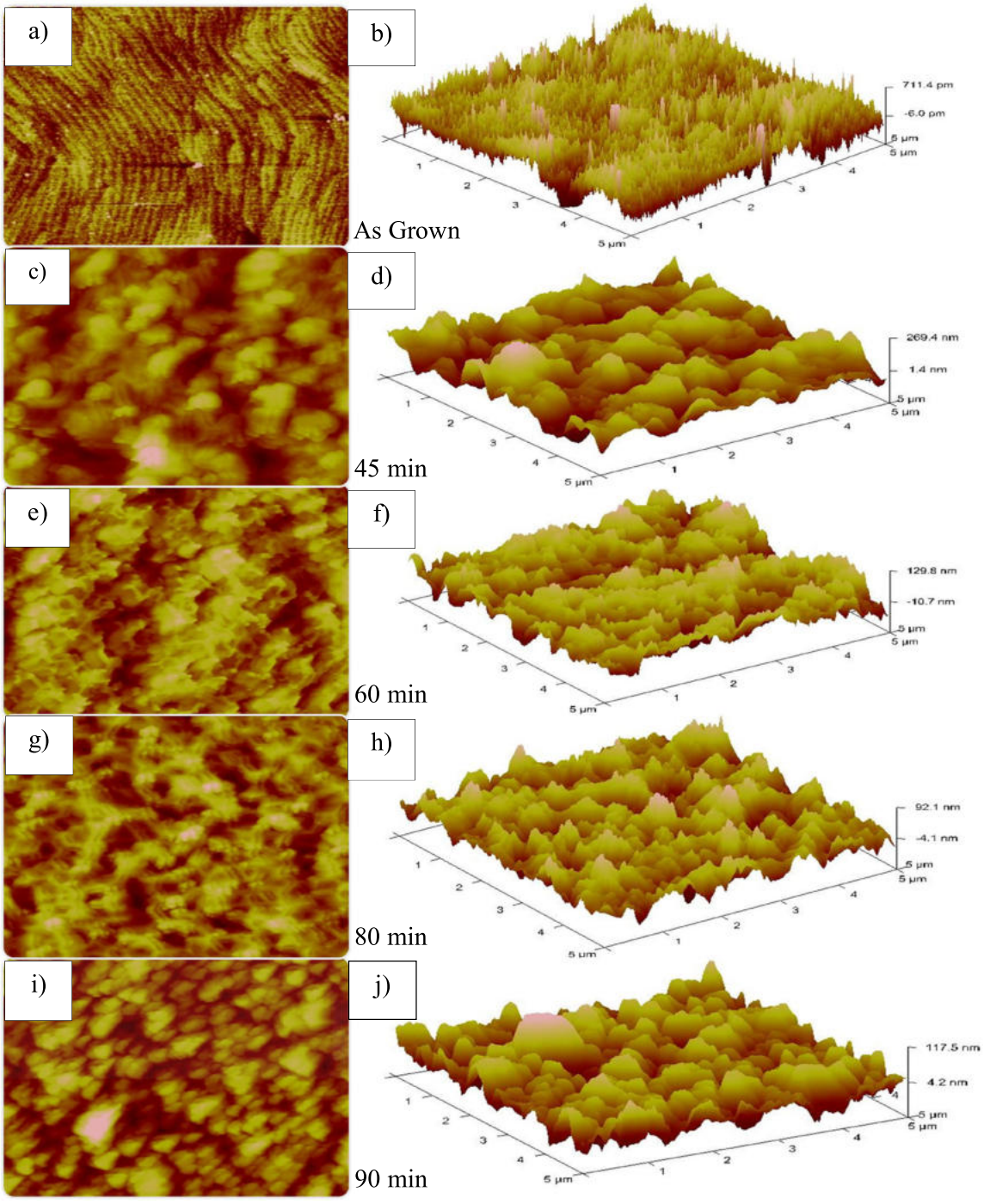

Fig. 4. 2D (a, c, e, g, i) and 3D (b, d, f, h, j) AFM micrographs of as grown and porous GaN under different etching duration.

defects in GaN crystals for both as-grown and porous samples, namely for N_{screw} and N_{edge}, are graphically depicted in Fig. 8, as calculated using the following Eqs. (6) and (7), respectively. [31,32]

$$N_{screw} = \frac{\beta^2{}_{(0002)}}{4.35 \times b^2{}_{screw}} \quad (6)$$

and

$$N_{edge} = \frac{\beta^2(10\bar{1}2)}{4.35 \times b^2{}_{edge}} \quad (7)$$

where N_{screw}, N_{edge}, $\beta(0002)$, $\beta(1012)$, b_{screw}, and b_{edge} are the screw dislocation density, edge dislocation density, ω-scan FWHM of (0002) plane, ω-scan

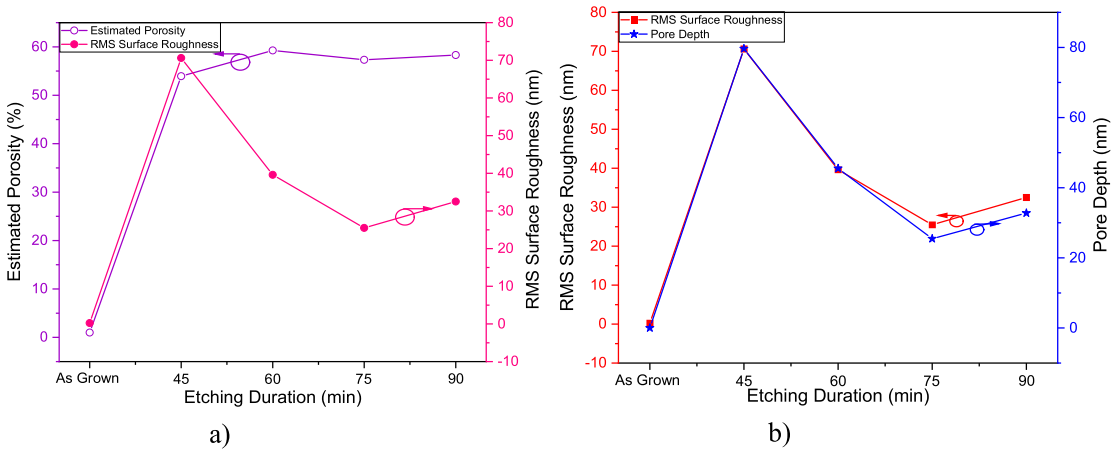

Fig. 5. The correlation of etching duration of porous of GaN sample and (a) estimated porosity with RMS surface roughness, (b) RMS surface roughness with pore depth.

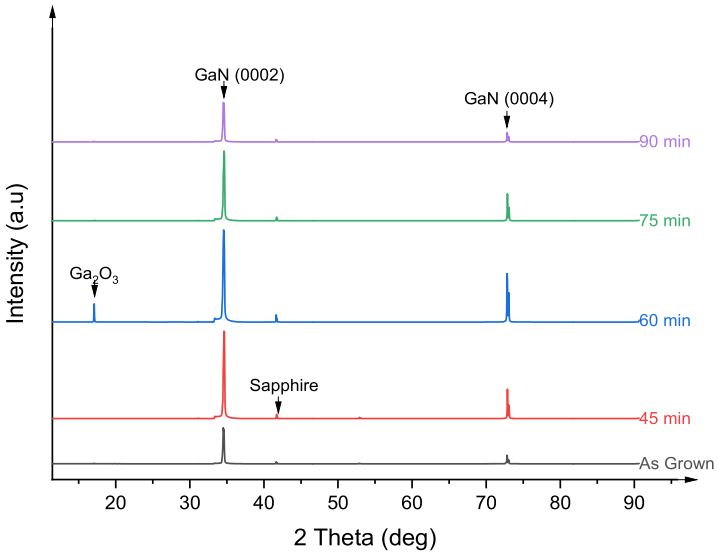

Fig. 6. HR-XRD of 2θ scan of as grown and porous Si-doped GaN at different etching durations.

Table 1. Peak position, FWHM and interplanar spacing HR-XRD of as grown and porous Si-doped GaN.

	0002		$10\bar{1}2$		d_{hkl}	
Sample	Peak (°)	FWHM (°)	Peak (°)	FWHM (°)	0002	$10\bar{1}2$
As Grown	17.664	0.0832	24.169	0.1088	0.2539	0.18819
45 min	17.195	0.0856	24.104	0.1110	0.2606	0.1886
60 min	17.273	0.0860	24.095	0.1115	0.2594	0.1887
75 min	17.123	0.0831	24.133	0.1085	0.2616	0.1884
90 min	17.650	0.0822	24.241	0.1109	0.2541	0.1876

FWHM of $(10\bar{1}2)$ plane, c-type Burger's vector, and a-type Burger's vector, respectively.

According to the mixed dislocation, which combined the N_{screw} and N_{edge}, all porous samples demonstrated a dislocation density that was significantly greater than that of the as-grown samples. This analysis demonstrated that this approach has caused a slight defect in the GaN crystals. Nonetheless, the values of N_{screw} and N_{edge} for each sample remained within the range suggestive of the high crystalline quality of GaN, which was characterised by the dislocation densities ranging from 10^5 to 10^8.[33] The values of N_{edge} were significantly higher than the values of N_{screw} for all samples, which were also observed by another research.[20]

The optical characteristics of the Si-doped GaN samples were analysed using Raman spectroscopy. Fig. 9(a) illustrates the Raman spectrum extending

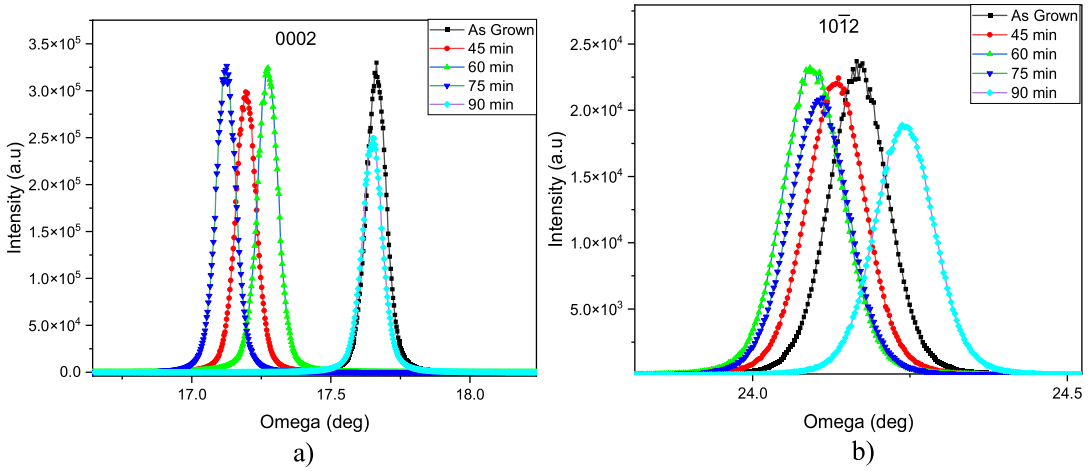

Fig. 7. HR-XRD of as grown and porous Si-doped GaN at different etching durations of a) of ω scan mode of 0002 and b) 10$\bar{1}$2.

Table 2. Lattice parameter, and dislocation density of HR-XRD analysis of as grown and porous Si-doped GaN.

	Lattice parameter		Dislocation density (cm^{-2})		
Sample	c (Å)	a (Å)	N_{screw} (x 10^8)	N_{edge} (x 10^8)	N_{total} (x 10^8)
As Grown	5.077	3.236	1.88	7.92	9.80
45 min	5.212	3.156	1.89	8.66	10.6
60 min	5.189	3.174	1.93	8.64	10.6
75 min	5.232	3.136	1.77	8.38	10.1
90 min	5.082	3.212	1.83	8.35	10.2

from 350 to 850 $cm^{-1,}$ and Fig. 9(b) displays the E_2 (high) and E_1 (TO) focused ranges. The identical phonon detected in Si-doped GaN exhibited varying intensities, specifically involving E_2 (high), E_1 (TO), and A_1 (LO). All phonon modes agreed with the Raman selection rules of wurtzite GaN.[26] Table 3 presents the peak positions, peak shifts, and relative intensities of all Si-doped samples etched under different etching durations. No peak shift was observed in the E_2 (high) phonon mode, showing that all porous samples etched under varying durations exhibited no stress change compared to the as-grown samples. The absence of the displacement of positive and negative charges within the unit cells could likely account for the E_2 vibration mode being classified as non-polar.[34] Relative intensity is observed in all porous samples, as depicted in Fig. 10.

The 60-min sample has the highest intensity, while the as-grown sample displayed the lowest intensity. The 45-min sample has a higher surface roughness based on the RMS surface roughness measurement in AFM. Nonetheless, the Raman spectra have shown that the highest surface roughness would not ensure the highest intensity of Raman analysis. This could be attributed to the significant lattice and thermal mismatches between the substrates and the epitaxial layer, resulting in increased defect density and

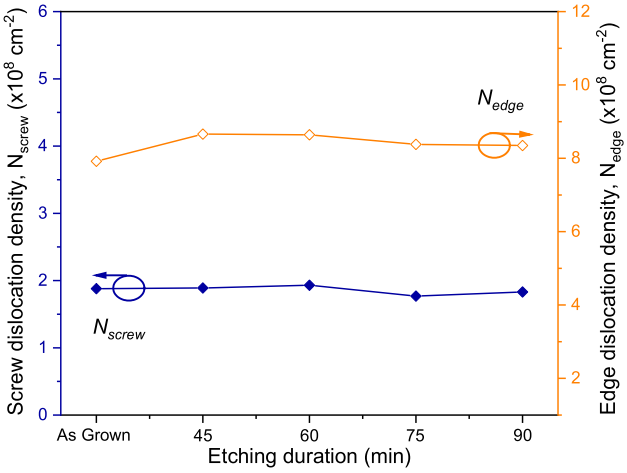

Fig. 8. The correlation of screw dislocation, edge dislocation and etching durations.

substantial biaxial stress, which in turn influenced the phonon scattering frequency.[34] Nonetheless, the accumulation of excessive etching residues on the porous surface may be a contributing factor to the deterioration of light scattering from the pore side walls.[19]

The as-grown and 60-min samples were chosen to undergo the I-V measurement for comparison. Fig. 11(a) shows the I-V characteristic graph of

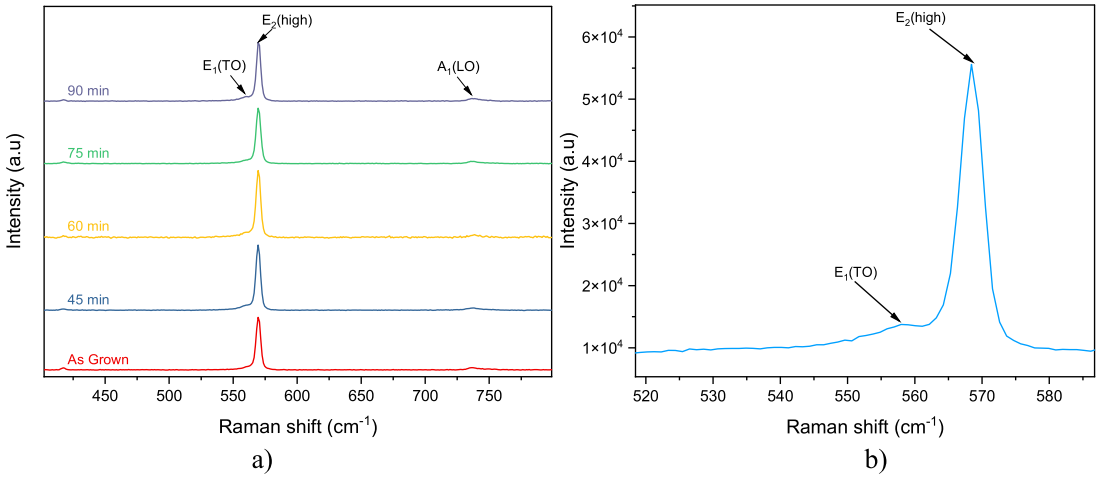

Fig. 9. The Raman spectra of as grown and porous Si-doped GaN samples etched under different durations of (a) full spectra and (b) short spectra focused on E_2 (high) and E_1 (TO).

Table 3. Peak position, intensity, peak shift, and relative intensity of Raman analysis of Si-doped GaN samples.

	E_2 (high)			A_1(LO)		E_1(TO)
Sample	Peak position (˚)	Intensity (a.u)	Relative intensity	Peak position (˚)	Peak shift (˚)	Peak position (˚)
As Grown	569.47	40298.17	1.00	736.57	–	–
45 min	569.47	49940.33	1.24	737.59	1.02	–
60 min	569.47	51230.85	1.27	738.61	2.04	–
75 min	569.47	42460.09	1.05	735.55	1.02	560.06
90 min	569.47	45013.93	1.12	736.57	–	560.06

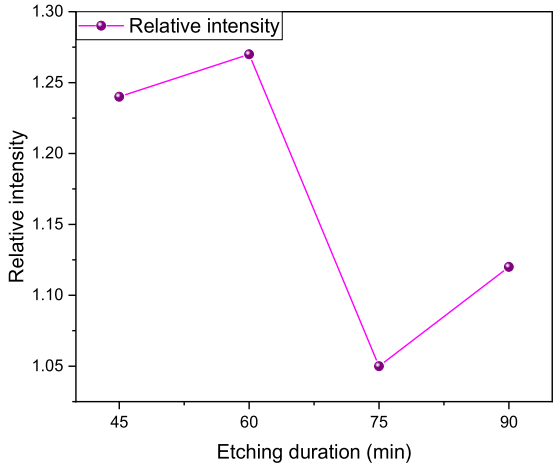

Fig. 10. Relative intensity of porous Si-doped GaN under different etching durations subjected to as grown for E_2 (high) phonon mode.

Si-doped GaN samples under the illumination of a room and dark environment. The dark and photo currents for Si-doped GaN-based MSM photodetectors were measured under room light and dark conditions, respectively. The porous sample has a considerably larger current at 5 V than the as-grown sample. The same phenomenon is observed under different light illuminations, as illustrated in Fig. 11(b) and as listed in Table 5.

Under light illumination at different wavelengths (469.0, 560.3, 577.0, and 632.9 nm), the photocurrent response of the etched samples showed a significant increase, demonstrating the photoconductive behaviour of the MSM photodetector. The highest photocurrent was observed in the 60-min etched sample, particularly at shorter wavelengths of blue illumination, indicating enhanced carrier generation and separation due to the increased surface area and porous structure. The increased photocurrent after etching could be attributed to the higher number of active sites for photon absorption, which enhanced carrier excitation and collection at the metal-semiconductor junction.[21] However, the current gain of the porous sample, as presented in Table 4, is slightly lower than the as-grown sample under all light illuminations, which has less current generated per photon, indicating limited sensitivity and responsiveness.[35]

The dark current of the as-grown sample exhibited a relatively low value, indicating minimal leakage current and a high-quality Schottky contact formation between Pt and GaN. However, after the sample underwent 60 min of etching, the dark current was increased, suggesting the introduction of additional defect states and surface states that may have contributed to the increased carrier recombination

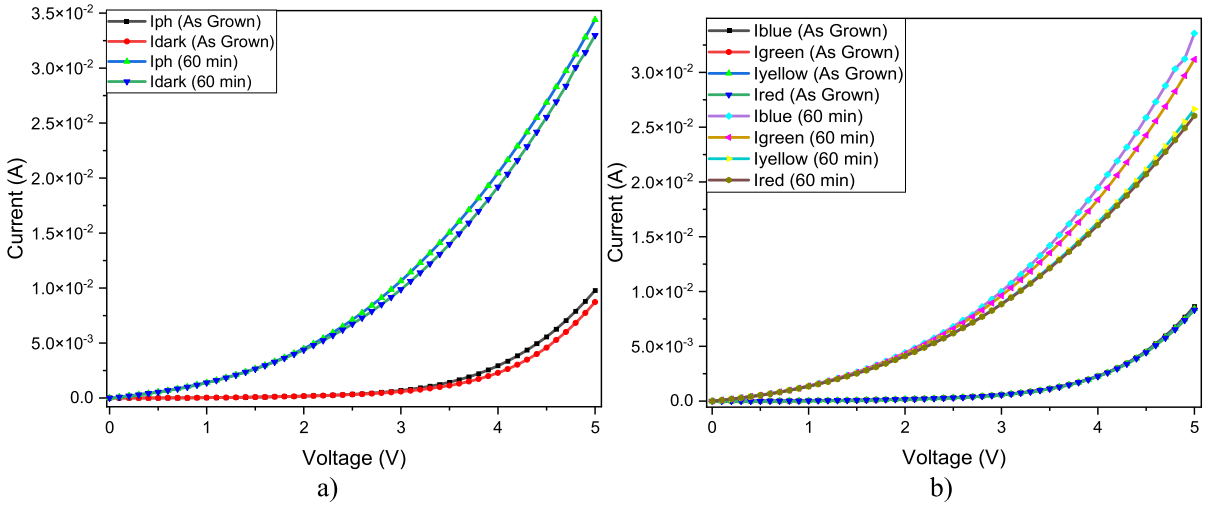

Fig. 11. I-V characteristics of fabricated MSM photodetector on as grown and porous Si-doped GaN sample under (a) photo and dark illumination, (b) blue, green, yellow and red illumination.

Table 4. Current and Current Gain of I-V characteristic of Si-doped GaN MSM photodetector.

Sample	Current at 5V (A)	Current Gain at 5V (A)	Ideality factor, (n)	SBH (eV)
As Grown (photo)	0.979×10^{-2}	1.121	40.155	0.7040
As Grown (dark)	0.873×10^{-2}		40.151	0.7037
60 min (photo)	3.440×10^{-2}	1.043	40.176	0.5745
60 min (dark)	3.298×10^{-2}		40.176	0.5743

Table 5. Current at 5V of as grown and porous Si-doped GaN sample under blue, green, yellow and red illumination.

Environment	Wavelengths (nm)	Sample	Current at 5V (A)	Current Gain at 5V (A)	Ideality factor, (n)	SBH(eV)
blue	469.0	As Grown	0.865×10^{-2}	0.991	40.155	0.7039
green	560.3		0.843×10^{-2}	0.966	40.155	0.7041
yellow	577.0		0.843×10^{-2}	0.966	39.853	0.7043
red	632.9		0.832×10^{-2}	0.953	40.164	0.7047
blue	469.0	60 min	3.356×10^{-2}	0.976	40.176	0.5746
green	560.3		3.118×10^{-2}	0.906	40.585	0.5863
yellow	577.0		2.664×10^{-2}	0.774	40.172	0.5750
red	632.9		2.603×10^{-2}	0.757	40.172	0.5750

and tunnelling effects.[36] The ideality factor (n) was observed to be higher in the etched sample compared to in the as-grown sample. This observation suggested the presence of additional charge transport mechanisms, such as trap-assisted tunnelling and defect-related recombination.[36] The Schottky barrier height (SBH) of the 60-min sample was relatively low, indicating efficient carrier transport at the metal-semiconductor interface. The post-etching enhancement in photocurrent across all wavelengths confirmed that porosity has played a crucial role in improving light absorption and carrier transport.

Conclusion

The Hg-HPVL-assisted ACPEC etching of GaN films was conducted in this study using a KOH electrolyte solution at various etching durations (45, 60, 75, and 90 min) under low temperature conditions. The findings revealed notable effects of etching duration on the porous morphology, as well as on the structural and optical properties of the samples. The surface morphology exhibited nanocoral-like and nanotunnel-like pore shapes, alongside multilayer structures. The AFM analysis further demonstrated significantly enhanced surface roughness among the etched samples compared to among the as-grown GaN samples, which also tallied with the porosity in the FESEM images. The XRD result showed that the dislocation density was in an acceptable range. Meanwhile, the optical properties of the samples, as assessed using Raman spectroscopy, indicated a substantial improvement in intensity in all porous samples in the E_2 (high) phonon mode. The fabricated device of the MSM photodetector for porous samples showed a higher current at 5 V compared to the as-grown samples in illuminated environments. Although the etching process introduced additional

structural defects, such as increased dislocation density and dark current, the nanostructured porous GaN samples demonstrated improved performance in terms of light absorption and photogenerated current under UV illumination. Their enhanced surface area and porous morphology promoted more efficient photon trapping, leading to a net increase in photocurrent. These improvements could particularly be beneficial for MSM photodetector applications. Therefore, the term "enhanced performance" in this work refers specifically to the functional optoelectronic response, rather than the overall structural perfection. In summary, the utilisation of low-cost Hg-HVPL-assisted ACPEC etching method at low temperatures has proved to be effective for fabricating porous structures with significant enhancements, in terms of porosity, surface roughness, and optical properties compared to as-grown samples. Thus, this method would be suitable for the fabrication of porous GaN-based photodetectors.

Acknowledgment

The authors express their gratitude to the Ministry of Higher Education (MOHE) through the Fundamental Research Grant Scheme (FRGS/1/2022/STG07/UITM/02/1) and the Institute of Graduate Studies UiTM for providing financial support. Appreciation was also extended to Universiti Teknologi MARA Cawangan Pulau Pinang for their contributions and support, as well as access to workstation facilities.

Authors' declaration

- Conflicts of Interest: None.
- We hereby confirm that all the Figures and Tables in the manuscript are mine/ours. Furthermore, any Figures and images that are not mine/ours have been included with the necessary permission for republication, which is attached to the manuscript.
- No animal studies are present in the manuscript.
- No human studies are present in the manuscript.
- Ethical Clearance: The project was approved by the local ethical committee at Universiti Teknologi MARA.

Authors' contributions

This study was carried out in cooperation with all researchers including experiment preparation, collecting data, analysis data, writing, checking and translating. The work of the first author N.I.N.I was writing the full manuscript, experiment preparation, collecting data and analysis data. A.M, R.R, and A.F.A.R were responsible experiment preparation, collecting data and checking the manuscript. M.D.J.O and N.M.A were responsible for translating the manuscript. The researchers read and agreed on the final reference.

Data availability statement

The data supporting the findings of this study are available from the corresponding author upon reasonable request.

Funding statement

This research was funded by the Ministry of Higher Education (MOHE) through the Fundamental Research Grant Scheme (FRGS/1/2022/STG07/UITM/02/1) and the Institute of Graduate Studies (IPSiS) UiTM (Kod Tabung: 250001040001) for providing financial support.

References

1. Samir E, El-Sagheer AM, Joudakaszis S. The structure, morphology, and optoelectronic properties of silicon nanowires decorated with GaN and Ag for single nanowire solar cell applications. Phys Rev B Condens Matter. 2024 Aug 15;687:416050. https://doi.org/10.1016/j.physb.2024.416050.
2. Li D, Han D, Chen Y, Hong Y, Duan Q, Wang H, *et al.* GaN/rGO nanocomposite gas sensor for enhanced NH_3 sensing performances at room temperature. Sens Actuators B Chem. 2024 Mar 15;403:135209. https://doi.org/10.1016/j.snb.2023.135209.
3. Poonia R, Bhat AM, Periasamy C, Sahu C. A highly sensitive nano gap embedded AlGaN/GaN HEMT sensor for Anti-IRIS antibody detection. Micro Nano Struct. 2022 Sep 1;169:207342. https://doi.org/10.1016/j.micrna.2022.207342.
4. Abbas IA, Kadhm AJ. Study the structural properties of porous silicon and their applications as thermal sensors. Baghdad Sci J. 2024 Mar 4;21(3):1086. https://doi.org/10.21123/bsj.2023.4097.
5. Khan MA, Rao MV. Gallium nitride (GaN) nanostructures and their gas sensing properties: a review. Sensors (Basel). 2020 Jul 13;20(14):3889. https://doi.org/10.3390/s20143889.
6. Huo Q, Shao Y, Wu Y, Zhang B, Hu H, Hao X. High quality self-separated GaN crystal grown on a novel nanoporous template by HVPE. Sci Rep. 2018 Feb 16;8(1):3166. https://doi.org/10.1038/s41598-018-21607-3.
7. Choi HW, Chua SJ, Raman A, Pan JS, Wee AT. Plasma-induced damage to n-type GaN. Appl Phys Lett. 2000 Sep 18;77(12):1795–7. https://doi.org/10.1063/1.1311605.
8. Li X, Liang Z, Wang F, Xu Y, Liu Z, Liang Y, *et al.* Effects of contactless photoelectrochemical reaction on repair of etching damage in GaN SBD. Mater Sci Semicond Process. 2024 Nov 15;183:108756. https://doi.org/10.1016/j.mssp.2024.108756.

9. Meyers V, Rocco E, Hogan K, Tozier S, McEwen B, Mahaboob I, *et al.* Removal of dry-etch-induced surface layer damage from p-GaN by photoelectrochemical etching. J Electron Mater. 2020 Jun;49:3481–9. https://doi.org/10.1007/s11664-020-07986-2.
10. Razali NS, Abd Rahim AF, Hassan NS, Radzali R, Mahmood A, Sabki SN, *et al.* Hexagonal enhanced porous GaN with delayed integrated pulse electrochemical (iPEC) etching. Int J Nanoelectron Mater. 2024 Oct 2;17(4):521–8. https://doi.org/10.58915/ijneam.v17i4.1278.
11. Awaid TJ, Ayal AK, Farhan AM, Sando MS, Chin LY. Effect of electrolyte composition on structural and photoelectrochemical properties of titanium dioxide nanotube arrays synthesized by anodization technique. Baghdad Sci J. 2020 Dec 1;17(4):1183. https://doi.org/10.21123/bsj.2020.17.4.1183.
12. Mahmood A, Hassan Z, Ahmed NM, Yam FK, Chuah LS, Mokhtar M, *et al.* Structural and optical studies of undoped porous GaN prepared by Pt-assisted electroless etching. Mater Sci Forum. 2016 Apr 6;846:358–65. https://doi.org/10.4028/www.scientific.net/MSF.846.358.
13. Díaz DJ, Williamson TL, Adesida I, Bohn PW, Molnar RJ. Morphology and luminescence of porous GaN generated via Pt-assisted electroless etching. J Vac Sci Technol B. 2002 Nov 1;20(6):2375–83. https://doi.org/10.1116/1.1521428.
14. Nor Izaham NI, Mahmood A, Abd Rahim AF, Mukhtar NM, Johan Ooi MD, Ahmed NM. The characterization of nanostructured GaN prepared via low temperature photoelectrochemical etching at different etching period. J Electr Electron Syst Res. 2024;25(1):108–12. https://doi.org/10.24191/jeesr.v25i1.012.
15. Vajpeyi AP, Chua SJ, Tripathy S, Fitzgerald EA, Liu W, Chen P, *et al.* High optical quality nanoporous GaN prepared by photoelectrochemical etching. Electrochem Solid-State Lett. 2005 Feb 10;8(4):G85. https://doi.org/10.1149/1.1861037.
16. Quah HJ, Lim WF, Hassan Z, Radzali R, Zainal N, Yam FK. Effects of ultraviolet-assisted electrochemical etching current densities on structural and optical characteristics of porous quaternary AlInGaN alloys. Arab J Chem. 2019;12(8):3417–30. https://doi.org/10.1016/j.arabjc.2015.10.003.
17. Massabuau FC, Griffin PH, Springbett HP, Liu Y, Kumar RV, Zhu T, *et al.* Dislocations as channels for the fabrication of subsurface porous GaN by electrochemical etching. APL Mater. 2020 Mar 1;8(3). https://doi.org/10.1063/1.5142491.
18. Youtsey C, Adesida I, Bulman G. Highly anisotropic photoenhanced wet etching of n-type GaN. Appl Phys Lett. 1997;71(15):2151–2153. https://doi.org/10.1063/1.11936513.
19. Lim WF, Hassan Z, Ahmed NM, Quah HJ. Porous formation in p-type gallium nitride films via 50 Hz operated alternating current-assisted photo-electrochemical etching in methanol–sulfuric acid solution. J Electrochem Soc. 2018;165(10):H620. https://doi.org/10.1149/2.0591810jes.
20. Quah HJ, Ahmed NM, Hassan Z, Lim WF. Surface alteration of planar P-type gallium nitride to porous structure using 50 Hz alternating current-assisted photo-electrochemical etching route. J Electrochem Soc. 2016 May 20;163(8):H642. https://doi.org/10.1149/2.0361608jes.
21. Garg M, Tak BR, Rao VR, Singh R. Giant UV photoresponse of GaN-based photodetectors by surface modification using phenol-functionalized porphyrin organic molecules. ACS Appl Mater Interfaces. 2019 Mar 27;11(12):12017–26. https://doi.org/10.1021/acsami.8b20694.
22. Sohimee SN, Hassan Z, Ahmed NM, Foong LW, Jin QH. Effect of different UV light intensity on porous silicon fabricated by using alternating current photo-assisted electrochemical etching (ACPEC) technique. J Phys Conf Ser. 2018;1083(1):012034. https://doi.org/10.1088/1742-6596/1083/1/012034.
23. Radzali R, Zainal N, Yam FK, Hassan Z. Characteristics of porous GaN prepared by KOH photoelectrochemical etching. Mater Res Innov. 2014;18:S6–412. https://doi.org/10.1179/1432891714Z.000000000989.
24. Daud ANM, Radzali R, Mahmood A, Hassan Z, Abd Rahim AF, Malik MF, *et al.* enhancement of structural and optical characteristics of nanostructured InGaN using electrochemical etching. Int J Nanoelectron Mater. 2023 Dec 26;16(December):347–59. https://doi.org/10.58915/ijneam.v16iDECEMBER.416.
25. Syuhadah N, Razali M, Farhanah A, *et al.* Morphological, structural and optical characteristics of porous GaN fabricated by UV-assisted electrochemical etching. Solid State Phenom. 2020;301:3–11. https://doi.org/10.4028/www.scientific.net/SSP.301.3.
26. Mahmood A, Hassan Z, Rahim AF, Radzali R, Ooi MD, Ahmad N. Enhancing performance of porous Si-doped GaN-based MSM photodetector using 50 Hz ACPEC. J Phys Conf Ser. 2020;1535:012006. https://doi.org/10.1088/1742-6596/1535/1/012006.
27. Zhang Z, Zhang L, Liu Z, *et al.* Foam-like GaN: Study on the controlled tuning of pore size by R group change in amino acid etchant and its ultra-high photocurrent response. Vacuum. 2022 Jan;196:110779. https://doi.org/10.1016/j.vacuum.2021.110779.
28. Lee S, Mishkat-Ul-Masabih S, Leonard JT, *et al.* Smooth and selective photo-electrochemical etching of heavily doped GaN:Si using a mode-locked 355 nm microchip laser. Appl Phys Express. 2017 Jan 1;10(1):011001. https://doi.org/10.7567/APEX.10.011001.
29. Harrington GF, Santiso J. Back-to-Basics tutorial: X-ray diffraction of thin films. J Electroceram. 2021 Dec;47(4):141–63. https://doi.org/10.1007/s10832-021-00263-6.
30. Ramesh M, Nagaraja HS. Effect of current density on morphological, structural and optical properties of porous silicon. Mater Today Chem. 2017 Mar 1;3:10–4. https://doi.org/10.1016/j.mtchem.2016.12.002.
31. Qu S, *et al.* Influence of the growth temperature of AlN buffer on the quality and stress of GaN films grown on 6H-SiC substrate by MOVPE. J Alloys Compd. 2010;502(2):417–22. https://doi.org/10.1016/j.jallcom.2010.04.185.
32. Christiansen S, Albrecht M, Strunk HP. Defect structure of epitaxial GaN films determined by transmission electron microscopy and triple-axis X-ray diffractometry. Philos Mag A Phys Condens Matter Struct Defects Mech Prop. 1998;77(4):1013–25. https://doi.org/10.1080/01418619808221225.
33. Hellman ES. Internet journal nitride semiconductor research. Mater Res. 1999;2:1–0. https://doi.org/10.1557/S1092578300000387.
34. Zeng Y, Ning J, Zhang J, Jia Y, Yan C, Wang B, *et al.* Raman analysis of E_2 (high) and A_1 (LO) phonon to the stress-free GaN grown on sputtered AlN/graphene buffer layer. Appl Sci. 2020 Dec 9;10(24):8814. https://doi.org/10.3390/app10248814.
35. Sze SM, Li Y, Ng KK. Physics of Semiconductor Devices. John Wiley & Sons; 2021 Mar 19.
36. Chen J, Huang CQ, Zhang X, Dong S, Yang X. A trap-assisted photomultiplication-type organic photodetector with high detectivity from visible to shortwave infrared light. IEEE J Electron Devices Soc. 2024 Dec 27. https://doi.org/10.1109/JEDS.2024.35233.

النقش الكهروضوئي المتناوب منخفض الحرارة لنتريد الغاليوم (GaN) من النوع n المطعم بالسيليكون: تصنيع البنى النانوية لتحسين أداء كاشف الضوء MSM

نور إيواني نور إزاهام[1]، أينورخيلاه محمود[2]، روسفاريزا رَدزالي[3]، ألهان فَرْحانة عبد الرحيم[3]، نور ميزاتول أزرا مختار[4]، مهاية تون دايانا يوهان أوي[5]، ناصر محمود أحمد[6]

[1]كلية العلوم التطبيقية، جامعة التكنولوجيا مارا، شاه علم، سلانغور، ماليزيا.
[2]قسم العلوم التطبيقية، جامعة التكنولوجيا مارا – فرع بينانغ، برماتانغ باوه، ماليزيا.
[3]دراسات الهندسة الكهربائية، كلية الهندسة، جامعة التكنولوجيا مارا – فرع بينانغ، برماتانغ باوه، ماليزيا.
[4]كلية العلوم الصحية، جامعة التكنولوجيا مارا – فرع بينانغ، كِبالا باتاس، ماليزيا.
[5]كلية الفيزياء، جامعة العلوم الماليزية، ميندن، ماليزيا.
[6]قسم هندسة الليزر والإلكترونيات الضوئية، كلية جامعة دجلة، بغداد، العراق.

الملخص

تتناول هذه الدراسة تصنيع نتريد الغاليوم (GaN) المسامي المطعَّم بالسيليكون باستخدام تقنية النقش الكهروضوئي بالتيار المتناوب منخفض الحرارة(ACPEC) ، وذلك عند مدد نقش مختلفة، بهدف تحسين أداء كاشفات الضوء من نوع MSM. جرى تحليل الخصائص البنيوية والبصرية لعينات الـ GaNالمسامية باستخدام مصباح بخار الزئبق عالي الضغط بقدرة 400 واط (Hg-HPVL) وإلكتروليت KOH بنسبة 4%، مع تيار متناوب شدته 100 mA وتردده 50 .Hz كما أُجريت قياسات التيار–الجهد (I-V) لتقييم أداء كاشف MSM المصنوع من عينات GaN المطلية بالبلاتين. كشفت صور المجهر الإلكتروني الماسح FESEM للعينات المنقوشة عن تكوّن مسام شبيهة بالشعاب المرجانية وأنفاق نانوية، بينما أظهرت طبوغرافيا مجهر القوة الذرية AFM زيادة ملحوظة في خشونة السطح مقارنة بالعينات غير المنقوشة. وأشار الفارق الطفيف بين متوسط عمق المسام وقيم خشونة الجذر التربيعي (RMS) إلى نجاح تشكيل بنية نانوية شبيهة بالشعاب المرجانية ذات عمق متجانس وموزع بانتظام. وأظهر تحليل مطيافية رامان للعينات المنقوشة حدوث انزياحات في أطوال موجات قمة(LO) A1 ، بالإضافة إلى زيادة في شدة قمة (high) E2 عبر مدد النقش المختلفة مقارنة بالعينات غير المنقوشة. كما أكّد تحليل حيود الأشعة السينية XRD وجود كثافة إزاحات على المحورين x و zفي جميع العينات. إضافةً إلى ذلك، كشفت قياسات I-V لكاشف MSM عن ارتفاع التيار في جميع العينات المسامية مقارنة بالعينات غير المنقوشة تحت ظروف بيئية متعددة. وتشير هذه النتائج إلى أن النقش الكهروضوئي بالتيار المتناوب منخفض الحرارة يُعدّ نهجًا فعالًا في تصنيع نتريد الغاليوم المسامي ذي التيارات العالية، مما يجعله مناسبًا لتطبيقات كاشفات الضوء.

الكلمات المفتاحية: الحرارة المنخفضة، كاشف ضوئي MSM، البنى النانوية، كهروضوئي، كهروضوئي، نتريد الغاليوم المطعَّم بالسيليكون (Si-doped GaN).